

InterPUF: Distributed Authentication via Physically Unclonnable Functions and Multi-party Computation for Reconfigurable Interposers

Ishraq Tashdid¹, Tasnuva Farheen², Sazadur Rahman¹

¹University of Central Florida, Orlando, FL, USA, ²Louisiana State University, Baton Rouge, LA, USA
{ishraq.tashdid, sazadur.rahman}@ucf.edu¹, tfarheen@lsu.edu².

Abstract—Modern system-in-Packages (SiP) platforms are rapidly adopting reconfigurable interposers to enable plug-and-play chiplet integration across heterogeneous multi-vendor ecosystem. However, this flexibility introduces severe trust challenges, as traditional security countermeasures fail to scale or adapt in these decentralized, post-fabrication programmable environments. This paper presents INTERPUF, a compact, scalable authentication framework that transforms the interposer into a distributed root of trust. At its core, INTERPUF embeds a route-based differential delay Physical Unclonnable Function (PUF) across the reconfigurable interconnect and secures its evaluation using multi-party computation (MPC). The proposed architecture introduces only 0.23% area and 0.072% power overhead across diverse chiplets while preserving authentication latency within tens of nanoseconds. Simulation results using PyPUF confirm strong uniqueness, reliability, and modeling resistance, even under process, voltage, and temperature variations. By fusing hardware-based PUF primitives with cryptographic hashing and collaborative verification, INTERPUF enforces a minimal-trust model without relying on any centralized anchor.

Index Terms—Secure Heterogeneous Integration, Physically Unclonnable Function.

I. INTRODUCTION

Cost increases from IC manufacturing processes, shrinking technology nodes, and the growing complexity of integrated circuits have forced original equipment manufacturers (OEMs) to outsource parts of their design, integration, and fabrication to third-party vendors, contract foundries, and packaging facilities. In contrast, a full-custom ASIC allows a single design house to control specification, design, and manufacturing maximizing flexibility and trust [1] but at the cost of long development cycles and high non-recurring engineering (NRE) expenses. Foundry-provided process design kits (PDKs) mitigate these costs and improve yield but reduce design flexibility and security. Today's System-on-Chip (SoC) designs rely heavily on reusable IP blocks, making full custom design impractical. This reuse-driven paradigm has accelerated innovation and reduced both cost and time-to-market. The microelectronics industry is now extending this modular approach through heterogeneous integration, using chiplets, interposers, and advanced 2.5D/3D packaging [2]. In these system-in-package (SiP) architectures, pre-fabricated logic, memory, analog, and accelerator chiplets from diverse vendors are assembled on shared interposer platforms. Passive and active interposers [3]–[8] enable dense, high-bandwidth chiplet communication, while emerging reconfigurable inter-

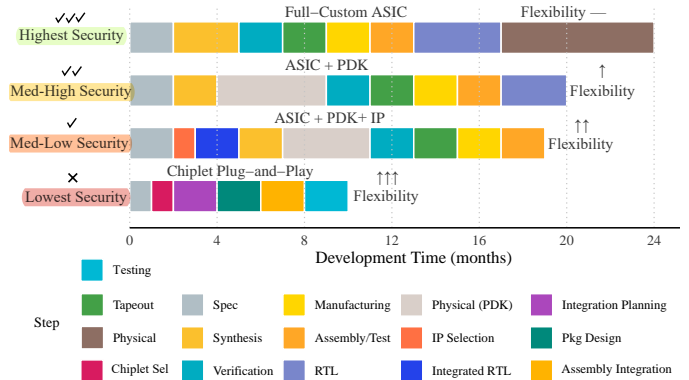


Fig. 1: Comparison of development time across design flows. Each bar illustrates the sequence and duration of design stages. As it evolves from full-custom to chiplet-based integration, redundant steps e.g., Register Transfer Level (RTL) design or physical implementation are reduced or eliminated, shortening time-to-market.

posers further enable plug-and-play integration [9]–[11]. With these programmable fabrics, designers can mix and match chiplets like lego blocks, extending product lifetimes through reconfiguration and rapidly prototyping new designs.

The transition to a horizontally distributed IC supply chain, involving multiple global entities, has introduced a range of security threats, including IP piracy, hardware Trojan insertion, counterfeiting, reverse engineering, and overproduction [12]. In contrast, earlier full-custom design flows kept specification, design, and fabrication in-house, preserving confidentiality and minimizing exposure to external risks [13]. As design and manufacturing responsibilities have shifted to outsourced foundries, IP vendors, and chiplet suppliers, the attack surface has expanded dramatically [14]. The threat model for each stage of the design flow is summarized in Table I. IP vendors may conceal malicious logic [13]; foundries can overproduce, reverse engineer, or tamper with layouts [15], [16]; and integrators must guard against counterfeit or reused chiplets [17]. Furthermore, many SoC-level defenses such as logic locking [13], IC metering [1], and scan-chain protections [18] do not directly apply to chiplet-based SiPs, where integrators cannot modify third-party components. *Each outsourcing step thus trades security assurance for faster design cycles, yielding a fragmented, minimal-trust supply chain.*

Reconfigurable interposer-based SiPs most starkly expose the speed–trust trade-off: programmability enables adaptive

TABLE I: Threat model across common design flows.¹

Design Flow	Entities Involved	Threat Models
Full-custom ASIC	Design house	Insider threat
ASIC+PDK	+ Foundry	+ Untrusted Foundry
ASIC+PDK+IP	+ Vendors	+ IP Piracy
Chiplet Plug-and-Play	+ Packaging	+ Chiplet Foundry

routing and interoperability yet centralizes attack surface [19]. Thus, the interposer must serve as a verifiable root of trust or modularity becomes systemic risk. Existing SiP trust schemes rely on centralized anchors (a trusted chiplet/port) [20], [21], creating bottlenecks and single points of failure; cryptographic handshakes add latency [22]; many MPC approaches still assume a central validator [23]; and interposer-centric RoTs remain fixed and don't scale across reconfigurable, multi-vendor meshes [24]. We therefore need distributed, scalable trust. MPC enables joint verification without revealing secrets [23], [25]–[27] and is proven at scale in software [28]–[30]. We propose INTERPUF: a decentralized, interposer-resident trust fabric that verifies authenticity via MPC while never exporting raw PUF outputs. Our main contributions follow.

- We propose INTERPUF, which embeds a differential, route-based delay PUF in the reconfigurable interposer and uses it as the SiP-wide root of trust.
- We design a protocol that secret-shares only stabilized tokens and chiplet encryption, enabling distributed accept/reject decisions without a central validator with raw challenge-response pairs (CRPs) never cross the boundary.
- Our hardware evaluation shows that INTERPUF achieves negligible interposer overhead below 0.23%, per-chiplet encryption overhead as low as 0.48%, and power under 0.072%, while maintaining fast authentication latency.
- Simulation results with PYPUF confirm strong PUF quality (uniformity ~ 0.5 , reliability 98%, uniqueness ~ 0.46), and machine-learning attacks achieve only random-guess accuracy ($\sim 47\%$), validating resilience.
- We analyze resilience to modeling, replay, probe, and Denial of Service (DoS) attacks under a sceptical-trust supply chain.
- To accelerate further research and facilitate industrial adoption, we will release our Verilog implementation, evaluation scripts, and benchmark data as open-source at our GitHub.

The paper is organized as follows: Sec. II reviews related work, Sec. III defines the threat model, and Sec. IV describes the architecture and operation of INTERPUF. Sec. V outlines the simulation flow, Sec. VI reports evaluation results, and Sec. VII analyzes resilience. Sec. VIII discusses limitations, and Sec. IX concludes.

II. BACKGROUND AND RELATED WORK

Authentication in heterogeneous multi-chiplet systems requires both architectural support and scalable trust. This section reviews prior work along three directions: ① advances

¹Here ‘+’ means addition along with the previous entries. For example, ASIC+PDK+IP design flow involves design house, foundry, and vendors while threat model includes insiders, untrusted foundry, and IP piracy. Common threats, such as, hardware Trojans; side-channel leakage, fault injection, test/DFT abuse, forged documentation, are omitted for space.

TABLE II: Contrast with Prior Authentication Approaches.

Method	Drawbacks	Advantages of INTERPUF
GATE-SiP [20]	TAP-based; susceptible to MITM	No TAP changes; robust against MITM
PQC-HI [22]	High computation cost; leakage under probing	low-overhead, distributed checks with strong signature hashing
SECT-HI [21]	Focuses test encryption; limits vendor flexibility	Supports both vendor and integrator security
SAFE-SiP [23]	Relies on a central hub; no single point of failure; scalable and efficient	Distributed validation;

TAP: Test Access Port. MITM: Man-in-the-Middle.

in heterogeneous integration and reconfigurable interposers enabling plug-and-play assembly; ② existing techniques for SiP security, which often rely on centralized anchors or heavy cryptography; and ③ delay-based PUFs, a compact primitives for unique hardware signatures, motivating INTERPUF.

A. Heterogeneous Integration and Reconfigurable Interposers

Heterogeneous Integration (HI) is the cornerstone of microelectronics in the post-Moore era by treating the interposer not as a passive carrier but as an active design resource that enables modularity at scale [31]. This modular approach reduces cost, improves yield, and shortens design cycles by reusing known-good dies across multiple products. However, today's interposers are mostly custom-designed for each system, limiting reuse and constraining agility [10]. In practice, most SiP interposers still employ fixed metal routing; truly reconfigurable routing meshes remain an active research direction rather than commodity practice [9]–[11], [32], [33]. By decoupling chiplet function from wiring, these techniques enable plug-and-play composition (late binding, binning, and field repair), but they also introduce new security challenges as highlighted next.

B. Challenges of Reconfigurable Interposers

Reconfigurable silicon interposers, while offering in-field programmability, also enlarge the attack surface. Unlike static interposers, their dynamic reprogrammability can introduce new runtime vectors for adversaries to exploit post-deployment [34], [35]. ① Adversaries may reconfigure the interposer to inject hardware Trojans or alter interconnect topologies to subvert system behavior [35], [36]. ② Moreover, unauthorized access to communication channels may hijack or reroute data flows across chiplets [36]. And, ③ covert side-channel leakage, enabled by dynamically reconfiguring signal paths to observe or modulate sensitive data [37]. Hence, ensuring provenance across evolving configurations, therefore, requires attestation of configuration state, secure firmware for the configuration controller, and lifecycle monitoring.

C. Existing Works and Their Drawbacks

Prior works (Tab. II) focus on static interposers via fabrication-time countermeasures, hardware primitives, and cryptographic protocols. Split manufacturing (SM) and network-on-interconnect (NoI) obfuscation conceal design information to impede reverse engineering [38]. SM's reliance

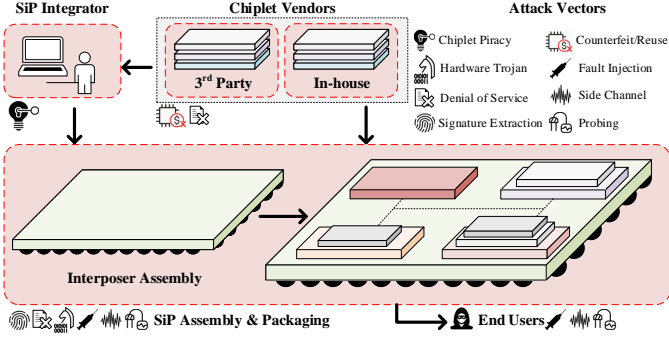


Fig. 2: SiP design flow and life-cycle. Untrusted and trusted parties are marked by red and green boxes, respectively.

on trusted back-end fabrication limits scalability and compromises yield, while NoI obfuscation complicates integration and validation [16]. Module-level approaches, e.g., Chiplet Hardware Security Modules (CHSM) and Chiplet Security IP (CSIP), provide authentication but at the cost of additional area and design complexity, and they (re)introduce single points of failure [14]. Researchers proposed post-quantum cryptographic authentication and encrypted test protocols [21], [22] that rely on centralized trust anchors and incur non-trivial latency overheads. Nonetheless, MPC-assisted frameworks [23] are typically coordinator-based. Moreover, none of these methods explicitly target reconfigurable interposers, where routing state can evolve over time (shown in Sec. II-A, II-B). Collectively, these limitations motivate an authentication primitive that is efficient, scalable, and trust-minimized/coordinator-free, and that is tailored to reconfigurable interposer fabrics.

D. Delay-based PUFs

Physical Unclonable Functions (PUFs) include several families: ① Arbiter PUFs, where challenge bits steer two matched delay paths and an arbiter records the race—yielding many challenge-response pairs (CRPs) but making them vulnerable to modeling and side-channel attacks when CRPs are exposed [39], [40]; ② Ring-oscillator (RO) PUFs, which compare oscillator frequencies and are well suited for FPGAs [41]; ③ Between-die delay PUFs, extending delay races across chips through bumps, vias, and package traces [42]; and ④ Interconnect PUFs, which embed races in interposer or routing fabrics for SiP authentication [43]. Arbiter PUFs typically chain 64–512 stages to build entropy. Delay-based PUFs are sensitive to process, voltage, temperature, and aging variations, which can be mitigated through majority voting, bit pre-selection, and lightweight error correction. Modeling attacks grow effective with large CRP exposure, while side channels (power, timing, EM) can leak responses; countermeasures include limiting CRPs, hashing challenges, and retaining raw responses on-chip.

III. THREAT MODEL AND ASSUMPTIONS

Our framework adopts a minimal-trust assumption in which no single actor in the heterogeneous integration flow is fully trusted [44]. The relevant actors are ① chiplet vendors (counterfeit or reused chiplets), ② the interposer/packaging foundry (tampering with routing fabrics, unauthorized reconfiguration,

interconnect probing), ③ system integrators (semi-honest or malicious misuse of authentication artifacts), and ④ end-users/field adversaries (runtime reconfiguration after deployment). Chiplets are treated as identity-bearing components with opaque internals; we do not verify internal functionality. Moreover, out-of-scope threats include malicious-by-design chiplets with functional Hardware Trojans; such cases require additional supply-chain defenses beyond our focus.

Parties participating in verification are at least semi-honest (follow the protocol but may be curious). Enrollment occurs in a trusted environment or procedure to obtain reference data (e.g., golden challenge-response information). Raw PUF responses are not exported during operation, and reference use avoids exposing raw CRPs. Attack capabilities considered include ① cloning/reuse and substitution, ② replay and chosen-challenge attempts aimed at modeling the PUF, ③ probing or rerouting on the interposer to extract or bias signals, and ④ configuration tampering and denial-of-service (DoS) by abusing reprogrammability. Side-channel attacks (power, EM, timing) are acknowledged but full side-channel hardening is beyond the scope of this work and discussed as a limitation. Given the adversary model, our security objectives include

- Authenticate chiplets without exposing raw CRPs.
- Resist modeling, replay, and cloning attacks even under partial compromise of the supply chain.
- Maintain robustness to moderate noise, environmental variations, and aging effects.
- Scale efficiently with mesh size and chiplet count in large SiP assemblies.

IV. SYSTEM OVERVIEW

In this section, we present the INTERPUF architecture which leverages interposer-integrated routing, compact delay chains, and distributed chiplet wrappers to enable scalable authentication in multi-chiplet systems. Sec. IV-A elaborates on the high-level system overview, illustrated in Fig. 3 while IV-B discusses the system-level operation, shown in Fig. 4.

A. Architecture

This subsection provides a high-level overview of our architecture which will be made publicly available on GitHub after publication. While a PUF is inherently a physical phenomenon that cannot be fully captured through logical code, we approximate its behavior here and later present a detailed simulation-based model in Sec. V.

1. INTERPOSER MESH: At the heart of the system lies a Manhattan mesh interconnect, the plug-and-play base proposed in [9] for 2.5D interposer-based integration. The mesh is composed of router tiles, each supporting bidirectional links to adjacent tiles. This topology is both cost-effective and reconfigurable, minimizing wiring overhead while maintaining sufficient flexibility for large-scale integration. Every router tile includes a compact switchbox that determines the direction of signal flow. The simplicity of this design not only reduces area and power but also allows low-overhead PUF integration at router boundaries. As a result, the interconnect itself

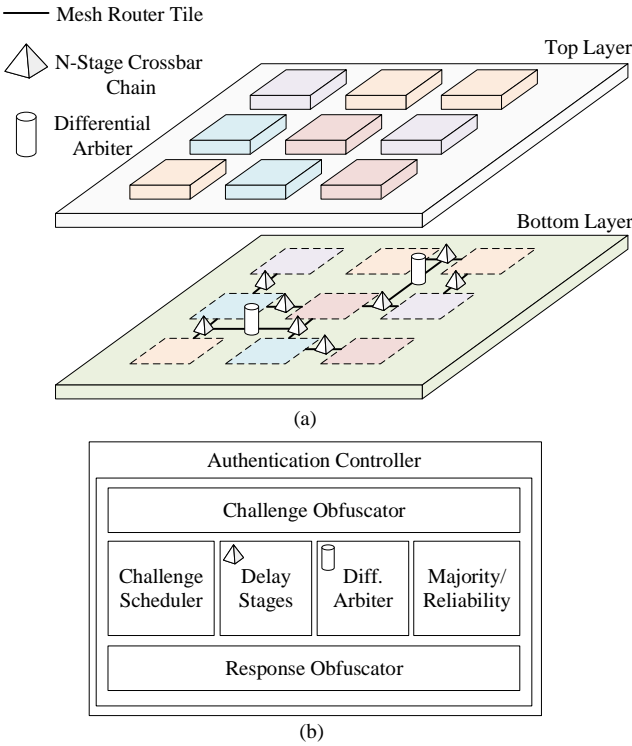


Fig. 3: Architecture of INTERPUF. (a) Physical organization of the system, where the bottom layer integrates the interconnect mesh with embedded N -stage crossbar chains and differential arbiters, and the top layer hosts chiplets interconnected through the fabric. (b) Authentication controller, which manages challenge hashing, scheduling, differential arbitration, majority/reliability voting, and response hashing.

becomes an active participant in system-level authentication rather than a passive wiring fabric.

1.A PROCESS: In INTERPUF, each router tile embeds a small “ N -Stage” crossbar-based delay chain, which is the base of the PUF. A pair of neighbor routes is selected per challenge, forming an “A-path” and a “B-path” across the mesh. The delays along these two paths are compared using a differential arbiter located at the sink. Sec. IV-B-2 shows an example of this path pair. Since process variation ensures unique delay characteristics per device, the arbiter’s outcome serves as a device-specific response. Repeating this process across challenges yields a rich response space that is tightly bound to the physical structure of the interconnect. Therefore, we instantiate many neighbour or identical length source–sink pairs and, per pair, each stable race contributes one bit, so aggregating across pairs and permutations yields a 256- or 512-bit route digest without requiring 256/512 dedicated stages in a single path. Only challenges that pass stability thresholds across PVT. All PUF stages (delay elements and switchboxes) reside on the interposer, chiplets act only as sources/sinks, and the arbiter is time-multiplexed at the interposer edge. For scale, a 16×16 mesh with typical source–sink distances of 20–30 hops and 40–80 path pairs, each with 8 path permutations, produces

320–640 candidate bits; after stability filtering (~ 60 –80%), a 256 bit digest is readily realized without on-chip stages.

1.B GOLDEN-FREE INTERPOSER SELF-CHECK To detect route tampering without any external golden reference, the interposer exploits the fact that a crossed switchbox setting introduces more delay than a straight setting [45]. Consider an N -stage differential path race between two routes (A and B) connecting neighboring chiplets (See Fig. 4-2.1). We begin from a symmetric baseline where both routes are configured all-cross (Fig. 4-2.2). Suppose A arrives earlier (Fig. 4-2.3), indicating the winner of the race. Then we change the configuration of route B by flipping the first Z stages from cross to straight (keeping all stages on route A as cross) and evaluate the arbiter outcome again under majority voting (Fig. 4-2.4). The smallest Z at which B consistently wins is recorded as the threshold Z^* for that {source, sink} pair.

Intuitively, Z^* captures how much delay “headroom” exists between the two nominally identical routes. Honest, un-tampered fabrics produce tightly clustered Z^* values across different pairs. So, any hidden delay (e.g., a stealth insertion, unintended extra buffering, or re-route) along a route shifts its threshold, making its Z^* , a clear outlier from the population mean Z_{avg} . During enrollment, the controller collects the vector of thresholds Z^* across many local pairs and stores in the designers secure repository (detail discussed in Sec. IV-B-2). In the field, periodic re-checks recompute Z^* and flag routes whose thresholds drift beyond the allowed band, providing golden-free integrity monitoring. If a dormant Trojan was inactive at enrollment [46], later periodic checks (performed opportunistically at boot or during low-load windows) still surface its effect when it activates, as the corresponding Z^* deviates sharply from Z_{avg} .

2. AUTHENTICATION CONTROLLER: In INTERPUF, authentication is not pushed down to the chiplets via dedicated wrappers, ensuring that even if third-party vendors performs denial-of-service, the scheme cannot be bypassed since authentication remains a centralized task enforced at the interposer level. To ensure this, the authentication controller embedded in the interconnect is composed of several low-overhead but coordinated components as shown in Fig. 3.

- A *challenge scheduler*, which orchestrates and delivers challenges across the mesh fabric.
- A *challenge obfuscator*, which transforms challenges to conceal any correlations, increasing modeling resistance.
- Distributed delay stages and differential arbitrators, which evaluate timing races induced by challenges.
- A *majority/reliability unit*, which repeats evaluations, suppresses noise, and filters unstable challenges. This improves validity against PVT variation, and also against adversarial perturbations, such as hardware Trojans that may selectively trigger faults in a single instance [47].
- A *response obfuscator*, which hashes or encodes final response bits into short authentication tokens before exposing them externally, ensuring that raw delay information is never directly observable.

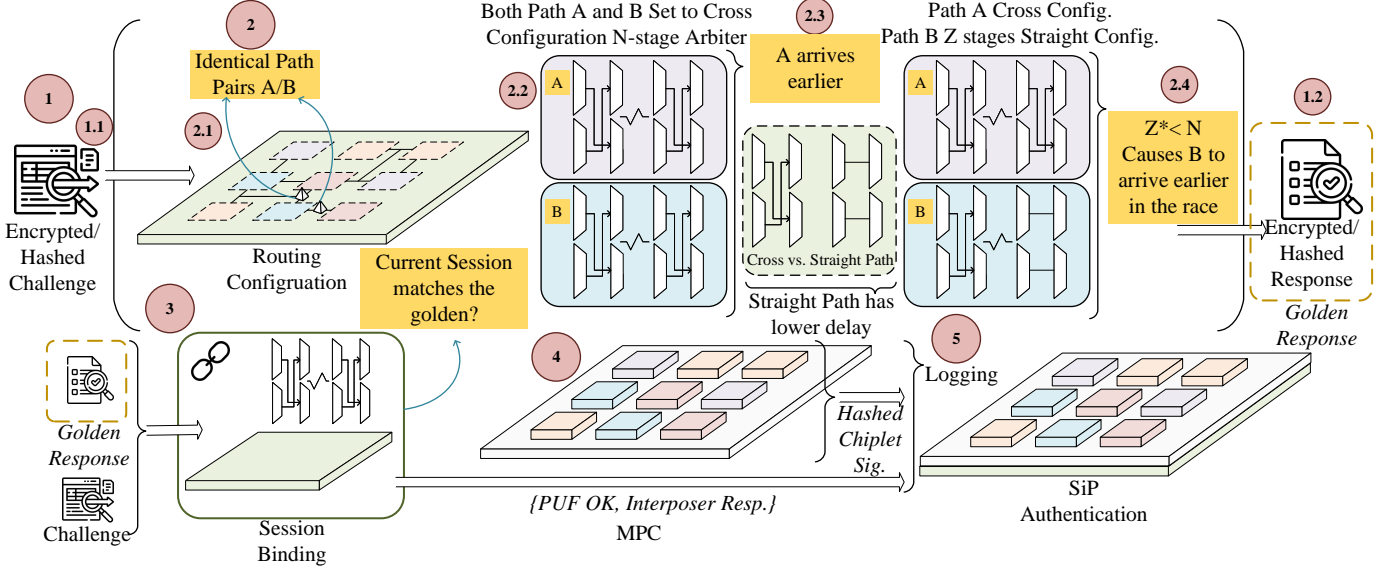


Fig. 4: Operation flow of INTERPUF.

This interconnect-level controller establishes a scalable two-layer trust hierarchy. The interposer fabric itself becomes the first line of defense, validating routing integrity and guaranteeing a trustworthy communication backbone. On top of this, individual chiplets contribute their cryptographic signatures, which are evaluated only after the interconnect has been secured. By clearly decoupling the compact interconnect authentication from heavier chiplet-level encryption (discussed in Section IV-B), the system achieves both efficiency and robustness without duplicating logic across every chiplet.

B. Operation

We present an interposer-centric flow in Fig. 4 in which (i) the interposer exposes only a golden route digest derived from its differential-delay PUF and (ii) each chiplet binds its identity to that digest at enrollment. At runtime, authentication is realized as a constant-round two-party MPC between the interposer (verifier) and a chiplet (prover).

0. NOTATION: Interposer \mathcal{I} ; chiplets $\mathcal{C} = \{C_1, \dots, C_N\}$. Let \mathbf{ch} be a routing challenge, EPOCH a session identifier, and NONCE a fresh per-session value. SHA256 denotes SHA-256; HKDF is HMAC-based KDF (Key Derivation Function). Concatenation is \parallel . PRK is Pseudo-Random Key.

1. CHALLENGE-RESPONSE: During enrollment, for a curated challenge set and PVT corners, \mathcal{I} evaluates differential paths with K -fold repetition and majority vote (Fig. 4-1.1). Responses with flip-rate below τ are retained. The accepted bitstring is hashed to a fixed-length golden route digest, R^* , with the help of a designer chiplet (Fig. 4-1.2).

$$R^* = \text{SHA256}(\text{stable_PUF_bits}).$$

Raw CRPs never leave \mathcal{I} ; only R^* is exported for binding.

2. ENROLLMENT: Enrollment runs on standard Automated Test Equipment (ATE) at the Outsourced Semiconductor Assembly and Test (OSAT). The ATE executes a signed test program, and the tester host is paired with a Hardware Security Module (HSM), possibly a random designer chiplet, that attests tester identity, gates cryptographic operations, and produces

signed logs. But both parties need to exchange hash to confirm the security of the process. For a curated challenge set and representative PVT corners, the interposer evaluates many races, and hashes the admitted bits to produce the golden route digest R^* . Optional helper data (if used) are stored as non-sensitive metadata in on-device Non-Volatile Memory (NVM). Each digest is bound to traceability fields (device identifier, wafer, lot), and the HSM signs a per-device enrollment manifest (device ID, digest set/version, trace metadata, tester attestation) that is uploaded to the designer’s secure repository. The OSAT retains only pass/fail and non-sensitive logs. Separately, each chiplet C_i binds its local identity to the interposer’s PUF via a one-time commitment

$$G_i = \text{SHA256}(\text{ID}_i \parallel \text{SIG}_i \parallel R^* \parallel \text{ENROLLTAG}),$$

where ID_i is a device-local identifier and SIG_i is a vendor signature or silicon-resident secret attesting ID_i . Only G_i and trace metadata are provided to the integrator; $(\text{ID}_i, \text{SIG}_i)$ never leave C_i . The interposer stores G_i (and the signed manifest) in secure NVM.

3. SESSION BINDING: The interposer derives a per-session salt s from the golden digest R^* and the current context (\mathbf{ch} , EPOCH), and samples a fresh NONCE; both values are public within the session and bind all proofs to this interposer instance while preventing replay. Authentication proceeds only if the current challenge passes the PUF stability check ($\text{PUF_OK}=1$) (Illustrated in Fig. 4-3).

4. MPC: The goal is to decide if the chiplet holds identity material that reproduces G_i bound to R^* , and produce a per-session token tied to (s, NONCE) , without revealing either party’s secrets. Fig. 4-3 shows that in each run, the interposer supplies its private inputs (G_i, R^*) , the chiplet supplies its private inputs $(\text{ID}_i, \text{SIG}_i)$, and both parties use the public inputs $(s, \text{NONCE}, \text{PUF_OK})$. They execute two-party computation using Yao garbled circuits with Oblivious Transfer to evaluate a fixed circuit f_i , inspired by [23].

- The circuit first recomputes $G'_i = \text{SHA256}(\text{ID}_i \parallel \text{SIG}_i \parallel R^* \parallel \text{ENROLLTAG})$.
- It then sets b_i to true iff $G'_i = G_i$ and $\text{PUF_OK} = 1$.
- It finally derives a session token $T'_i = \text{SHA256}(G'_i \parallel s \parallel \text{NONCE})$. Only (b_i, T'_i) are revealed to the interposer.
- Concretely, the interposer garbles f_i and sends the garbled tables to the chiplet, provides input labels for (G_i, R^*) , and the chiplet obtains labels for $(\text{ID}_i, \text{SIG}_i)$ via OT.
- Both parties encode $(s, \text{NONCE}, \text{PUF_OK})$ as public inputs.
- The chiplet evaluates the garbled circuit and returns the garbled outputs, and the interposer decodes them to obtain (b_i, T'_i) and accepts only if $b_i = 1$.

This 2PC protocol completes in a constant number of rounds, independent of circuit depth.

5. LOGGING: Upon acceptance ($b_i=1$), the interposer may record $(i, \text{ch}, \text{EPOCH}, \text{NONCE}, T'_i)$ for audit and replay detection, while avoiding any storage of secret inputs. Because $T'_i = \text{SHA256}(G_i \parallel s \parallel \text{NONCE})$ and the salt s is derived fresh each session, tokens are unlinkable across sessions.

An impostor that lacks $(\text{ID}_i, \text{SIG}_i)$ bound to G_i and R^* cannot satisfy $G'_i = G_i$ inside the 2PC check and therefore cannot produce a valid T'_i . Token replay is ineffective because (s, NONCE) changes every session. Copying G_i alone is insufficient without the corresponding identity material. Throughout the protocol, neither G_i nor $(\text{ID}_i, \text{SIG}_i)$ is revealed. For any subset $\mathcal{S} \subseteq \{1, \dots, N\}$, the interposer runs f_i independently for each $i \in \mathcal{S}$ (in parallel when available) and then applies a local policy predicate to the resulting bits $\{b_i\}_{i \in \mathcal{S}}$ (e.g., quorum) to produce the final decision.

V. MODELING AND SIMULATION METHODOLOGY

This section presents a complete, interposer-aware simulation flow designed to mirror the register-transfer-level (RTL) implementation. We employ PYPUF [48] to reproduce parametric PUF behavior, integrate standard machine-learning frameworks for modeling attacks, and introduce pre- and post-processing layers that truly emulate the interconnect transformations and hashing wrappers observed in our RTL.

A. Design–Faithful System Abstraction

The hardware architecture is based on a Manhattan-style mesh, where each router and interconnect contributes to the PUF’s effective stage depth. In simulation, this is abstracted as the sum of tile sites and horizontal/vertical links, matching the RTL logic. Our default grid size of four yields a stage count consistent with the synthesizable mesh-based design. Each simulated chip instantiates an XOR-of- K arbiter family (with $K \geq 4$) to reflect the nonlinear aggregation introduced in RTL by multiple chains and parallel arbiters. Where the RTL uses tapped feedback to introduce feed-forward complexity, the simulator mimics this with lifted challenge features (pairwise interactions between chosen tap indices). This ensures that

the separation and nonlinearity effects captured in silicon are faithfully approximated in the software model.

The interconnect wrapper is modeled in three stages, aligned with how the RTL routes and perturbs challenge bits: (i) permutation of stage indices to emulate reordering by routers, (ii) sparse polarity flips to reflect wiring inversions and mode switches, and (iii) a sparse, invertible binary mixing matrix to capture weak coupling among neighboring links. Each router configuration deterministically defines these transformations, ensuring that every interconnect setting produces a consistent, device-specific challenge mapping. The mapping remains invertible by construction, ensuring that entropy is not artificially added or lost, thereby mirroring the RTL’s structure-preserving routing logic.

B. Measurement Pipeline and PVT Realism

CRPs are generated in large batches across multiple simulated devices to represent chip-to-chip variability. In hardware, inter-chip differences arise from uncontrollable process variation; in simulation, each chip is seeded independently to induce distinct delay biases. Likewise, interconnect diversity is introduced by random router configurations per challenge batch. To reflect operating conditions realistically, we incorporate Process, Voltage, and Temperature (PVT) effects as low-probability response flips. This models metastability, supply noise, and temperature-dependent delay shifts. Each challenge is evaluated multiple times, and a majority combiner, implemented with the same repetition depth as the RTL, produces a stable bit. Challenges are scored by their stability, and only the most reliable subset is retained, which mirrors enrollment in actual deployments where marginal CRPs near the decision boundary are discarded, ensuring that the dataset passed to the adversary matches what would realistically be exposed by deployed hardware.

C. Controlled Interfaces and Digest

In line with our RTL, challenges are not applied directly to the delay chain but first passed through an invertible linear transformation over GF(2). This hashing layer preserves entropy while removing fixed alignment between the external challenge and the internal stage basis, preventing straightforward modeling attacks. In simulation, we apply the same principle: a random but invertible binary matrix transforms challenges before evaluation.

Raw PUF bits never leave the system unprotected. In RTL, a low-overhead hashing stage converts stabilized responses into authentication tokens; in simulation, we use a 32-bit diffusion-oriented combiner that outputs ± 1 symbols. Session-bound digest is applied only after reliability filtering, ensuring instability is never masked. As a result, external observers or attackers only see obfuscated tokens rather than raw race outcomes, faithfully mirroring the deployed hardware’s information flow.

D. Attacker Models and Training Protocols

To evaluate resilience, we consider both oracle and deployed modes. In the oracle mode, all protections are disabled, expos-

TABLE III: Design Area Overhead of the Interconnect routing and PUF in INTERPUF.

Design	Design Area (μm^2)	Interconnect Route Area (μm^2)	Overhead (%)
CVA6 [49]	345,755	812.0	0.23
NVDLA [50]	541,552	835.5	0.15
RISC-V [51]	1,309,680	790.1	0.06
Ariane [52]	1,431,536	868.3	0.06
OR1200 [53]	1,488,384	805.2	0.05

ing raw arbiter responses. This provides a conservative lower bound, allowing standard logistic regression on ϕ -mapped features to model plain arbiter structures. In more realistic configurations (parallel XOR chains, feature-lifted challenges, interconnect mixing), we train multilayer perceptrons with tanh activations sized to the challenge dimension. Training and testing datasets are fixed across experiments to maintain reproducibility. Also, when response tokenization is enabled, direct CRP modeling is not possible, by interface design. In these cases, reported attack accuracy is suppressed not due to modeling limitations but because the system interface simply withholds raw data. This mirrors deployment reality, where external entities never access the unprotected bitstream. Thus, all reported attack results under oracle mode represent strict worst-case bounds, while the deployed mode faithfully mirrors the RTL’s hardened interface.

E. Metric Computation

We evaluate three canonical PUF metrics: uniqueness (average Hamming distance between devices), uniformity (average fraction of ones per device), and reliability (agreement across repeated reads). Importantly, these are measured *before* tokenization, aligning with how RTL majority voters stabilize responses. When tokenized outputs are used, proxy measurements (bitwise disagreements across tokens) are adopted to maintain comparability, all reported in Sec. VI-E.

VI. EVALUATION

This section evaluates the practicality of INTERPUF by analyzing its area, timing, and power overhead and compared with other relevant solutions along with results for simulation presented in the previous section.

A. Experimental Setup

We implemented INTERPUF in Verilog and synthesized the design using Synopsys Design Compiler with the SAED 14 nm standard cell library. Post-synthesis netlists were used to extract power, area, and timing metrics. All experiments were conducted on a dual-socket Intel Xeon (Skylake) server equipped with 32 cores and 190 GB of RAM. The synthesized design was functionally verified and achieved timing closure at 3 GHz under typical PVT conditions.

B. Area Efficiency and Scalability

Area efficiency is one of the most critical enablers for security primitives in heterogeneous multi-chiplet systems. A security mechanism that consumes excessive silicon quickly becomes impractical at scale, where dozens of chiplets may

TABLE IV: Design Area Overhead of Chiplet Encryption (per-chiplet, with proposed changes).

Design	Design Area (μm^2)	Chiplet Encryption Area (μm^2)	Overhead (%)
CVA6 [49]	345,755	6,988.2	2.02
NVDLA [50]	541,552	7,192.1	1.33
RISC-V [51]	1,309,680	7,063.0	0.54
Ariane [52]	1,431,536	7,000.5	0.49
OR1200 [53]	1,488,384	7,108.0	0.48

TABLE V: Area Comparison with Recent Works.

Work	LUT Resource	FF	Area (mm^2)
SECT-HI [21]	–	–	5.11
PQC-HI (Kyber+Dilithium) [22]	76,999	49,993	–
PQC-HI (Kyber only) [22]	1,842	1,634	–
INTERPUF (1 chiplet)	1,915	1,160	0.0078
INTERPUF (32 chiplets)	61,280	37,120	0.2501

be integrated within a single package. The key advantage of INTERPUF lies in its architecture; rather than replicating costly encryption engines within each chiplet, authentication is embedded directly into the interconnect fabric. This design ensures that the majority of the security cost is a one-time expense at the SiP level, while the marginal per-chiplet overhead remains negligible.

Table III highlights this property, resulting in great area reduction. The routing fabric and embedded PUF together occupy less than $900 \mu\text{m}^2$, which translates to an overhead of only 0.05–0.23% depending on the SoC baseline. Importantly, this cost does not grow with the number of chiplets in the system: once the secure interconnect is in place, additional chiplets can be authenticated without increasing the routing area. In other words, the fundamental cost of interconnect-level security is fixed for the package, not per chiplet.

Moreover, summarized in Table IV, each chiplet must integrate an encryption core of roughly $7,000 \mu\text{m}^2$, leading to overheads in the range of 0.5–2.0% per design. While such costs may appear modest in isolation, they scale linearly with the number of chiplets. A 32-chiplet system would pay for 32 redundant encryption engines, wasting silicon that could otherwise be allocated to computation or memory. By eliminating these blocks, INTERPUF achieves nearly an order-of-magnitude reduction for large-scale systems.

The scalability advantage is further evident when comparing it with recent secure hardware solutions, as shown in Table V. For a single chiplet, INTERPUF requires only 0.0078 mm^2 , which is already an order of magnitude smaller than PQC accelerators and several times smaller than enclave-based schemes such as SECT-HI [21]. When scaled to 32 chiplets, the total overhead remains just 0.2501 mm^2 , which is still dramatically lower than competing solutions. This proves that, unlike most alternatives, INTERPUF does not collapse under scale: the security mechanism remains compact even for the most demanding chiplet counts.

Taken together, these results establish a compelling case for INTERPUF. It introduces a fixed, SiP-wide interconnect overhead of less than 1%, avoids the linear per-chiplet penalties of standalone encryption, and scales gracefully to dozens

TABLE VI: Power Overhead of Interconnect Routing in INTERPUF.

Design	Baseline Power (mW)	Interconnect Power (mW)	Overhead (%)
CVA6 [49]	12.896	0.0093	0.072
NVDLA [50]	185.140	0.0098	0.005
RISC-V [51]	59.164	0.0087	0.015
Ariane [52]	94.157	0.0102	0.011
OR1200 [53]	106.610	0.0091	0.009

TABLE VII: Power Overhead of Chiplet Encryption (per-chiplet, with proposed changes).

Design	Baseline Power (mW)	Chiplet Encryption Power (mW)	Overhead (%)
CVA6 [49]	12.896	0.2357	1.83
NVDLA [50]	185.140	0.2394	0.13
RISC-V [51]	59.164	0.2518	0.43
Ariane [52]	94.157	0.2463	0.26
OR1200 [53]	106.610	0.2485	0.23

of chiplets without exceeding the area budgets of modern SoCs. No prior work demonstrates this balance of efficiency and scalability, making INTERPUF uniquely suited for secure heterogeneous integration at scale.

C. Power Efficiency and Overhead Analysis

Power overhead is a critical consideration for security primitives in multi-chiplet systems, since any recurring cost directly impacts runtime energy budgets. Table VI shows that the interconnect routing and embedded PUF in INTERPUF consume less than 0.011 mW across all evaluated SoCs, corresponding to only 0.005%–0.072% overhead relative to baseline power budgets that already span tens to hundreds of milliwatts. This extremely low figure is not incidental, but stems directly from the architectural simplicity of the design. Unlike conventional cryptographic accelerators, INTERPUF avoids wide datapaths, deep pipelines, and heavy arithmetic. Instead, it relies on compact combinational logic and a handful of low-overhead sequential registers, leading to inherently low switching activity. As a result, the measured dynamic power falls into the sub-10 μ W range, well below typical SoC power variation margins, making the overhead effectively invisible in practice. Moreover, Table VII highlights the comparison with per-chiplet encryption blocks, which consume around 0.24 mW each, or 0.2%–2.0% overhead depending on the host design. Still scaling largely, even for typical open-source SoC/chiplets. This can be improved further with the inclusion of clock gating or repurposing the encryption core for functional use for the chiplets.

In comparison to other works, INTERPUF maintains its negligible footprint regardless of scale, and its compact logic is highly amenable to standard low-power techniques such as clock gating and operand isolation, which could reduce consumption even further. Other recent works, such as SECT-HI and PQC-HI, did not report power results, but given their millimeter-scale area and reliance on complex cryptographic primitives, their power overheads are expected to be significantly larger [21], [22]. Therefore, INTERPUF

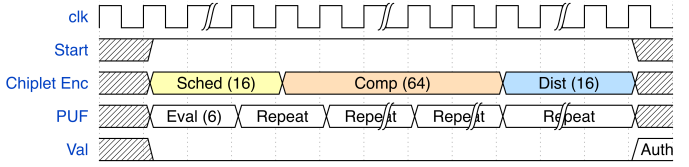


Fig. 5: Waveform diagram of authentication stages in INTERPUF. The interconnect PUF completes in 6 cycles and can be repeated multiple times within a single SHA-256 window (96 cycles). This ensures that interconnect validation is established as the root of trust before authentication.

provides a much better security solution with virtually negligible power overhead. Combined with its area efficiency, these results demonstrate that INTERPUF not only reduces silicon footprint but also ensures energy sustainability for secure heterogeneous integration.

D. Authentication Latency Breakdown

Authentication in INTERPUF proceeds in two tightly coupled stages: first, the interconnect fabric is authenticated using the embedded PUF, and then chiplet-level claims are validated using a SHA256 pipeline. This staged approach ensures that the interconnect, the communication backbone of the SiP, is established as the root of trust before chiplets are admitted into the system.

The interconnect authentication is extremely low-overhead, requiring only 6 cycles in total: one cycle for challenge scheduling followed by five cycles of PUF evaluation. At our 3 GHz operating frequency, this corresponds to roughly 2 ns. Because of its small footprint, the interconnect can be re-evaluated many times with virtually no penalty. For instance, during the 96 cycles required to compute a single SHA256 digest, the interconnect can be authenticated up to $96/6 \approx 16$ times. This allows repeated testing, majority voting for error suppression, and rotation of path configurations to increase modeling resistance, so the routing fabric is validated with high confidence before chiplet-level authentication begins.

Chiplet authentication is performed by transmitting hashed signatures that are validated through the SHA256 pipeline. This hashing stage requires 96 cycles in total, with 16 cycles for message scheduling and 64 cycles for compression rounds, followed by minor control overhead, resulting in less than 32 ns at 3 GHz. This process runs in parallel with ongoing interconnect validation, so by the time the chiplet digest is ready, the fabric has already been re-checked several times.

To bind each acceptance to the current PUF-derived session, we add a constant-round two-party computation (2PC) step (Yao garbled circuits with Oblivious Transfer). The online cost is dominated by sending one garbled circuit for a fixed function f_i (recompute SHA256 over the chiplet’s identity material and R^* , check equality with the stored commitment, then derive a session token) plus one batch of OT-extension messages, and finally revealing the outputs. With half-gates, the garbled size for this circuit is on the order of 0.6–1.0 MB at 128-bit security; on an on-package link of 32 GB/s this serializes in ≈ 20 –30 μ s, and on a 128 GB/s link in ≈ 5 –8 μ s.

TABLE VIII: Simulation metrics and modeling attack performance (4 chiplets, PYPUF).

Metric	Mean Value	Std. Dev.
Uniformity	0.4986	0.0028
Bias	0.0049	0.0037
Uniqueness (HD)	0.4648	0.0734
Reliability	0.9816	–
Intra-chip HD	0.0189	0.0008
Bit-aliasing	0.4986	–
Bit-flip sensitivity	0.5140	–
Modeling Attack (Accuracy)	0.4675	–
Modeling Attack (AUC)	0.4899	–

The round complexity is constant (two to three exchanges), so latency is bandwidth-bound rather than depth-bound. Thus the end-to-end per-chiplet path is

$$t_{\text{PUF}} \approx 2 \text{ ns}, \quad t_{\text{SHA256}} < 32 \text{ ns}, \quad t_{\text{2PC}} \approx 5\text{--}30 \mu\text{s},$$

with the nanosecond-scale PUF and hashing stages fully overlapped by the microsecond-scale 2PC. Multiple chiplets can be processed in parallel lanes while the interconnect continues periodic PUF self-checks.

The timing relationship between interconnect and chiplet authentication is illustrated in Fig. 5: the interconnect completes in a handful of cycles and can be repeated without bubbles, while the SHA256 pipeline handles chiplet signatures in a single digest round, and the constant-round 2PC adds a bounded, bandwidth-driven tail. This overlapping structure minimizes end-to-end latency and enforces a clear trust hierarchy, where the interconnect is first secured and chiplets are authenticated against it, providing both speed and robustness for scalable multi-chiplet systems.

E. PUF Simulation and Modeling Attack Results

To assess the robustness of the proposed INTERPUF, we conducted detailed simulations using the PYPUF framework (Tab. VIII). Five synthetic chip instances were generated under noise and process variation, with challenges transformed through router-based permutations and sparse flips. The evaluation confirmed strong statistical quality: average uniformity was 0.4986 ± 0.0028 , close to the ideal 0.5, and bias remained negligible at 0.0049. Reliability was high at 98.2%, and intra-chip Hamming distance across repeated queries was tightly bounded at 0.0189, confirming stability. Uniqueness, measured as mean inter-chip Hamming distance, was 0.4648, close to the ideal 0.5, while bit-aliasing stayed balanced at 0.4986. Bit-flip sensitivity averaged 0.5140, consistent with expected avalanche properties. To further test resilience, we applied a machine learning attack using logistic regression trained on 8000 CRPs and tested on 3000 unseen CRPs. The model achieved only 46.7% accuracy and an AUC of 0.4899, which is no better than random guessing (Fig. 6). This confirms that the transformation and hashing in INTERPUF significantly raise the difficulty of predictive modeling, preserving the trust-agnostic guarantees.

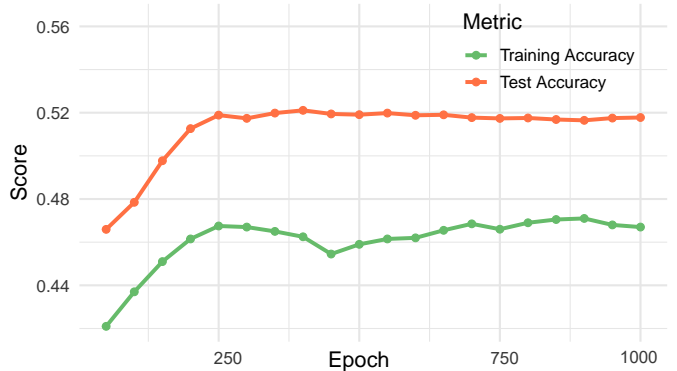


Fig. 6: Training curve for the modeling attack on INTERPUF, showing training and test accuracy over 1000 epochs. The training and test accuracy converges near 46% and 52% respectively, confirming resilience against learning models.

VII. SECURITY ANALYSIS

Security in heterogeneous multi-chiplet systems must be evaluated not only in terms of cryptographic strength, but also with respect to structural resilience against a wide spectrum of practical attacks. Because the interconnect serves as the communication backbone and chiplets themselves may originate from diverse vendors, an effective solution must withstand modeling attempts, replay and downgrade strategies, counterfeit component insertion, package-level tampering, denial-of-service, and side-channel exploitation. This section analyzes how the proposed architecture addresses these threats and demonstrates that robust authentication can be achieved with minimal overhead, while preserving scalability across many-chiplet systems.

A. Modeling and Reliability Attacks

Machine learning attacks on delay-based PUFs typically depend on access to large, stable sets of challenge-response pairs. In this design, two mechanisms frustrate such efforts. First, responses are always masked before being exposed, so attackers never see raw bit flips or stability patterns; second, effective challenges are permuted and masked differently in every session, preventing cross-session dataset aggregation. In addition, repeated evaluation with majority voting eliminates exploitable bias, while attempt gating limits the number of challenges an adversary can collect in practice. Together, these defenses sharply reduce the feasibility of constructing accurate predictive models, as seen in Fig. 6.

B. Replay, Challenge Modification

Authentication transcripts are bound to per-boot salts and session nonces, ensuring that the same top-level challenge never maps to the same internal state across power cycles. This property renders replay attacks ineffective and previously recorded transcripts are useless in future sessions. Any absence of expected responses or masking signals triggers rejection before chiplets are admitted. Modification attacks also render pointless due to SHA being extremely sensitive (Fig 7).

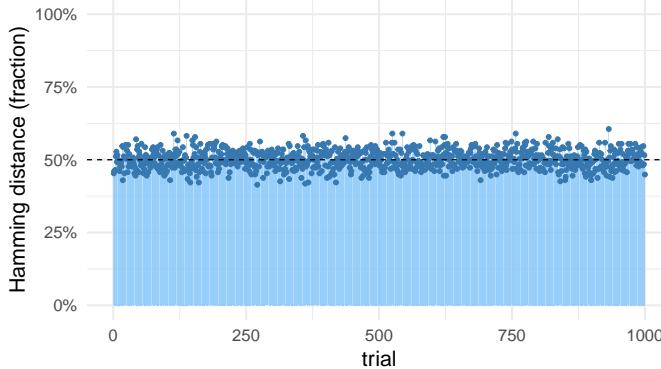


Fig. 7: Hamming distance distribution across 1000 trials. The plot demonstrates the stability of tokens, where the distance hovers around 50%, consistent with strong uniqueness.

C. Malicious or Counterfeit Chiplets

A rogue chiplet may attempt to spoof a valid identity or manipulate interconnect traffic to bias authentication. This system prevents such attacks by authenticating the interconnect before chiplets are considered. Because the backbone is secured first, any attempt to insert a counterfeit component occurs only after the interconnect has been verified multiple times. Once authenticated, genuine chiplets transmit hashed signatures that are validated against reference digests. Since replayed or fabricated signatures cannot pass verification without the correct secret context, malicious chiplets are effectively excluded.

D. Interposer and Package-Level Attacks

At the package level, an adversary could attempt to emulate valid delay paths by inserting programmable delays or rerouting signals through an interposer. However, the dynamic hashing of challenges and responses makes this infeasible: an attacker would need to replicate the per-boot remapping and masking keyed to device-unique values in real time, across many parallel evaluations. Repeated proofs within a single authentication session significantly increase path coverage, exposing even subtle deviations introduced by interposer-level manipulation.

E. Denial-of-Service and Throughput Abuse

Attackers may attempt to flood the system with challenges or intentionally stall transactions. Authentication logic enforces bounded attempts and cooldowns, preventing resource exhaustion. Because each interconnect proof completes in only a handful of cycles, the system can sustain frequent re-checks while maintaining throughput. Moreover, chiplet-level authentication runs concurrently with interconnect checks, ensuring that progress is not blocked even under partial denial-of-service attempts.

F. Side-Channels and Fault Injection

Since raw responses are never exposed, the information leaked through power or timing side-channels is already obfuscated and session-dependent. The logic itself is narrow, with constant-latency control paths and very low switching

activity, reducing exploitable leakage compared to large cryptographic blocks. Established countermeasures such as clock gating, operand isolation, and randomized re-check cadence can further strengthen resilience if required. Fault injection or environmental drift is mitigated by majority voting across repeated evaluations, allowing the system to reject inconsistent results and remain robust under variation.

G. Removal Attacks

In chiplet-based integration, an adversarial foundry or vendor may try to strip away authentication circuitry, bypass it, or insert malicious modifications. In INTERPUF, resilience is ensured by embedding authentication directly into the interconnect fabric rather than treating it as a detachable add-on. Because the security primitives are interwoven with routing and switching logic, there is no clean boundary to isolate and remove. Responses are further obfuscated and blended with normal interconnect activity, making them indistinguishable from functional signals. Any modification disrupts communication consistency and is quickly exposed during repeated challenge-response checks, making removal attacks significantly harder.

VIII. DISCUSSION AND LIMITATIONS

INTERPUF demonstrates several strengths. ① It achieves authentication with negligible overhead in both area and power, ② scales efficiently with growing chiplet counts, and ③ enforces a strict minimal-trust model by combining interconnect-level PUF proofs with chiplet-level hashed signatures. These properties make it low-overhead, practical, and well-suited for heterogeneous integration compared to prior centralized or heavyweight cryptographic approaches. Nonetheless, limitations remain. Our evaluation is confined to RTL-level prototypes and simulations, so real silicon validation under broader PVT variations, aging, and environmental stress is still required to confirm robustness over time. We have not yet built or evaluated an FPGA or silicon prototype; both are planned as next steps to validate functionality, quantify stability across PVT/aging, and measure end-to-end throughput and latency on hardware. A tape-out with controlled process corners and an FPGA-based emulation of the authentication controller are on our roadmap to complement the current synthesis and simulation-based results.

IX. CONCLUSION

INTERPUF introduces a low-overhead, interposer-resident authentication framework that combines delay-based PUFs with multi-party computation to enforce a strict minimal-trust model in heterogeneous chiplet systems. By embedding the root of trust in the interconnect and layering it with chiplet-level cryptographic signatures, the scheme achieves strong resilience against modeling, replay, and counterfeit attacks with negligible area and power overhead. Our RTL implementation and simulations confirm that the design scales efficiently with chiplet count, providing a practical path toward secure, reconfigurable system-in-package integration.

REFERENCES

- [1] M. Tehranipoor and C. Wang, *Introduction to hardware security and trust*. Springer Science & Business Media, 2011.
- [2] F. Sheikh et al., “2.5d and 3d heterogeneous integration: Emerging applications,” *IEEE Solid-State Circuits Magazine*, vol. 13, no. 4, pp. 77–87, 2021.
- [3] J. H. Lau, “Recent advances and trends in multiple system and heterogeneous integration with tsv interposers,” *IEEE Transactions on Components, Packaging and Manufacturing Technology*, vol. 13, no. 1, pp. 3–25, 2023.
- [4] D. Stow, Y. Xie, T. Siddiqua, and G. H. Loh, “Cost-effective design of scalable high-performance systems using active and passive interposers,” in *2017 IEEE/ACM International Conference on Computer-Aided Design (ICCAD)*, 2017, pp. 728–735.
- [5] I. Tashdid, V. Terry, J. Merkel, T. Farheen, and S. Rahman, “BeyondPPA: Human-inspired reinforcement learning for post-route reliability aware macro placement,” in *International Symposium on Machine Learning for CAD*, 2025.
- [6] I. Tashdid, D. Saiham, N. Anjum, T. Farheen, and S. Rahman, “Ecologic: Enabling circular, obfuscated, and adaptive logic via efpga-augmented socs,” *arXiv preprint arXiv:2508.04516*, 2025.
- [7] D. Saiham, M. Rabadi, D. Wu, and S. Rahman, “Can photonic interconnects be used for high-throughput memory access in the accelerators?” in *2025 IEEE/ACM International Symposium on Low Power Electronics and Design (ISLPED)*, 2025, pp. 1–7.
- [8] A. Ayes, E. G. Friedman, and M. Wolf, “Network-on-interposer co-design for heterogeneous chiplet-based integrated systems,” in *2025 IEEE International Symposium on Circuits and Systems (ISCAS)*, 2025, pp. 1–5.
- [9] Z. Li and D. Wentzlaff, “Lucie: A universal chiplet-interposer design framework for plug-and-play integration,” in *2024 57th IEEE/ACM International Symposium on Microarchitecture (MICRO)*, 2024, pp. 423–436.
- [10] F. Li, Y. Wang, Y. Cheng, Y. Wang, Y. Han, H. Li, and X. Li, “Gia: A reusable general interposer architecture for agile chiplet integration,” in *Proceedings of the 41st IEEE/ACM International Conference on Computer-Aided Design*, 2022, pp. 1–9.
- [11] B. Jiao, L. Xu, X. Yu, H. Yang, H. Zhu, Y. Wang, J. Zhu, D. Wen, L. Wang, J. Tao, C. Chen, Y. Han, Q. Liu, N. Sun, and M. Liu, “Fpia: Communication-aware multi-chiplet integration with field-programmable interconnect fabric on reusable silicon interposer,” *IEEE Transactions on Circuits and Systems I: Regular Papers*, vol. 71, no. 9, p. 4156–4168, 2024.
- [12] B. Shakya, M. Tehranipoor, S. Bhunia, and D. Forte, “Introduction to hardware obfuscation: Motivation, methods and evaluation,” in *Hardware Protection through Obfuscation*. Springer, 2017, pp. 3–32.
- [13] M. T. Rahman et al., “Defense-in-depth: A recipe for logic locking to prevail,” *Integration*, vol. 72, pp. 39–57, 2020.
- [14] N. V. et al., “ToSHI - towards secure heterogeneous integration: Security risks, threat assessment, and assurance,” *Cryptography ePrint Archive*, Paper 2022/984, 2022. [Online]. Available: <https://eprint.iacr.org/2022/984>
- [15] M. S. Rahman, H. Li, R. Guo, F. Rahman, F. Farahmandi, and M. Tehranipoor, “Ll-atpg: logic-locking aware test using valet keys in an untrusted environment,” in *2021 IEEE International Test Conference (ITC)*. IEEE, 2021, pp. 180–189.
- [16] S. Rahman et al., “Lle: Mitigating ic piracy and reverse engineering by last level edit,” in *International Symposium for Testing and Failure Analysis*, vol. 84741. ASM International, 2023, pp. 360–369.
- [17] F. Farahmandi, M. S. Rahman, S. R. Rajendran, and M. Tehranipoor, *CAD for hardware security*. Springer, 2023.
- [18] M. S. Rahman, A. Nahiyani, F. Rahman, S. Fazzari, K. Plaks, F. Farahmandi, D. Forte, and M. Tehranipoor, “Security assessment of dynamically obfuscated scan chain against oracle-guided attacks,” *ACM Transactions on Design Automation of Electronic Systems (TODAES)*, vol. 26, no. 4, pp. 1–27, 2021.
- [19] L. K. Biswas, M. S. M. Khan, N. Varshney, P. Craig, Y. Peng, J. Tang, and N. Asadizanjani, “Sample preparation to access interposer interconnects of advanced packaging for probing,” in *2025 IEEE Workshop on Microelectronics and Electron Devices (WMED)*. IEEE, 2025, pp. 1–4.
- [20] G. I. Haidar et al., “Gate-sip: Enabling authenticated encryption testing in systems-in-package,” in *Proceedings of the 61st ACM/IEEE Design Automation Conference*, ser. DAC ’24. New York, NY, USA: Association for Computing Machinery, 2024. [Online]. Available: <https://doi.org/10.1145/3649329.3656527>
- [21] G. I. Haidar et al., “Sect-hi: Enabling secure testing for heterogeneous integration to prevent sip counterfeits.”
- [22] M. S. Ul Islam Sami et al., “Pqc-hi: Pqc-enabled chiplet authentication and key exchange in heterogeneous integration,” in *2024 IEEE 74th Electronic Components and Technology Conference (ECTC)*, 2024, pp. 464–471.
- [23] I. Tashdid, T. Farheen, and S. Rahman, “Safe-sip: Secure authentication framework for system-in-package using multi-party computation,” in *Proceedings of the Great Lakes Symposium on VLSI 2025*, ser. GLSVLSI ’25. New York, NY, USA: Association for Computing Machinery, 2025, p. 391–396. [Online]. Available: <https://doi.org/10.1145/3716368.3735248>
- [24] M. Nabeel, M. Ashraf, S. Patnaik, V. Soteriou, O. Sinanoglu, and J. Knechtel, “An interposer-based root of trust: Seize the opportunity for secure system-level integration of untrusted chiplets,” no. arXiv:1906.02044, 2019, arXiv:1906.02044 [cs]. [Online]. Available: <http://arxiv.org/abs/1906.02044>
- [25] I. Tashdid, T. Farheen, and S. Rahman, “Authentree: A scalable mpc-based distributed trust architecture for chiplet-based heterogeneous systems,” 2025. [Online]. Available: <https://arxiv.org/abs/2508.13033>
- [26] M. S. Riazi, M. Javaheripi, S. U. Hussain, and F. Koushanfar, “Mpcircuits: Optimized circuit generation for secure multi-party computation,” in *2019 IEEE International Symposium on Hardware Oriented Security and Trust (HOST)*, 2019, pp. 198–207.
- [27] E. M. Songhorai, S. U. Hussain, A.-R. Sadeghi, T. Schneider, and F. Koushanfar, “Tinygarble: Highly compressed and scalable sequential garbled circuits,” in *2015 IEEE Symposium on Security and Privacy*, 2015, pp. 411–428.
- [28] J. Zhou, Y. Feng, Z. Wang, and D. Guo, “Using secure multi-party computation to protect privacy on a permissioned blockchain,” *Sensors*, vol. 21, no. 4, 2021. [Online]. Available: <https://www.mdpi.com/1424-8220/21/4/1540>
- [29] I. Zhou, F. Tofiq, M. Piccardi, M. Abolhasan, D. Franklin, and J. Lipman, “Secure multi-party computation for machine learning: A survey,” *IEEE Access*, vol. 12, pp. 53 881–53 899, 2024.
- [30] S. Halevi, C. Hazay, A. Polychroniadou, and M. Venkitasubramaniam, “Round-optimal secure multi-party computation,” *Journal of Cryptology*, vol. 34, no. 3, p. 19, May 2021. [Online]. Available: <https://doi.org/10.1007/s00145-021-09382-3>
- [31] J. H. Lau, “Chiplet heterogeneous integration,” in *Semiconductor Advanced Packaging*. Springer, 2021, pp. 413–439.
- [32] P. Ehret, T. Austin, and V. Bertacco, “Sipterposer: A fault-tolerant substrate for flexible system-in-package design,” in *2019 Design, Automation & Test in Europe Conference & Exhibition (DATE)*, 2019, pp. 510–515.
- [33] A. Tslioukos and V. F. Pavlidis, “A design methodology for thermal monitoring of reusable passive interposers with rtds,” *IEEE Transactions on Very Large Scale Integration (VLSI) Systems*, vol. 33, no. 7, pp. 1803–1815, 2025.
- [34] A. P. Johnson, S. Patranabis, R. S. Chakraborty, and D. Mukhopadhyay, “Remote dynamic partial reconfiguration: A threat to internet-of-things and embedded security applications,” *Microprocessors and Microsystems*, vol. 52, pp. 131–144, 2017.
- [35] R. S. Chakraborty, I. Saha, A. Palchaudhuri, and G. K. Naik, “Hardware trojan insertion by direct modification of fpga configuration bitstream,” *IEEE Design & Test*, vol. 30, no. 2, pp. 45–54, 2013.
- [36] S. Charles and P. Mishra, “A survey of network-on-chip security attacks and countermeasures,” *ACM Computing Surveys (CSUR)*, vol. 54, no. 5, pp. 1–36, 2021.
- [37] S. R. Bommana, S. Veeramachaneni, S. Ershad, and M. Srinivas, “Mitigating side channel attacks on fpga through deep learning and dynamic partial reconfiguration,” *Scientific Reports*, vol. 15, no. 1, p. 13745, 2025.
- [38] Y. Safari, P. Aghanoury, S. S. Iyer, N. Sehatbakhsh, and B. Vaisband, “Hybrid obfuscation of chiplet-based systems,” in *2023 60th ACM/IEEE Design Automation Conference (DAC)*, 2023, pp. 1–6.
- [39] J. W. Lee, D. Lim, B. Gassend, G. E. Suh, M. Van Dijk, and S. Devadas, “A technique to build a secret key in integrated circuits for identification and authentication applications,” in *2004 Symposium on VLSI circuits. Digest of technical papers (IEEE Cat. No. 04CH37525)*. IEEE, 2004, pp. 176–179.

- [40] D. Lim, J. W. Lee, B. Gassend, G. E. Suh, M. Van Dijk, and S. Devadas, “Extracting secret keys from integrated circuits,” *IEEE Transactions on Very Large Scale Integration (VLSI) Systems*, vol. 13, no. 10, pp. 1200–1205, 2005.
- [41] G. E. Suh and S. Devadas, “Physical unclonable functions for device authentication and secret key generation,” in *Proceedings of the 44th annual design automation conference*, 2007, pp. 9–14.
- [42] K. Rosenfeld, E. Gavas, and R. Karri, “Sensor physical unclonable functions,” in *2010 IEEE international symposium on hardware-oriented security and trust (HOST)*. IEEE, 2010, pp. 112–117.
- [43] L. Yu, X. Wang, F. Rahman, and M. Tehranipoor, “Interconnect-based puf with signature uniqueness enhancement,” *IEEE Transactions on Very Large Scale Integration (VLSI) Systems*, vol. 28, no. 2, pp. 339–352, 2019.
- [44] A. Stern, H. Wang, F. Rahman, F. Farahmandi, and M. Tehranipoor, “Aced-it: Assuring confidential electronic design against insider threats in a zero-trust environment,” *IEEE Transactions on Computer-Aided Design of Integrated Circuits and Systems*, vol. 41, no. 10, pp. 3202–3215, 2021.
- [45] Y. Tamir and H.-C. Chi, “Symmetric crossbar arbiters for vlsi communication switches,” *IEEE Transactions on Parallel and Distributed Systems*, vol. 4, no. 1, pp. 13–27, 1993.
- [46] M. Mazeika, D. Hendrycks, H. Li, X. Xu, S. Hough, A. Zou, A. Rajabi, Q. Yao, Z. Wang, J. Tian, Y. Tang, D. Tang, R. Smirnov, P. Pleskov, N. Benkovich, D. Song, R. Poovendran, B. Li, and D. Forsyth, “The trojan detection challenge,” in *Proceedings of the NeurIPS 2022 Competitions Track*, ser. Proceedings of Machine Learning Research, M. Ciccone, G. Stolovitzky, and J. Albrecht, Eds., vol. 220. PMLR, 28 Nov–09 Dec 2022, pp. 279–291. [Online]. Available: <https://proceedings.mlr.press/v220/mazeika23a.html>
- [47] M. A. Bokor Siddik and S. H. Alam, “Puf-based hardware trojan: Design and novel attack on encryption circuit,” in *2023 International Conference on Electrical, Computer and Communication Engineering (ECCE)*, 2023, pp. 1–5.
- [48] N. Wisiol, C. Gräbnitz, C. Mühl, B. Zengin, T. Soroceanu, N. Pirnay, K. T. Mursi, and A. Baliuka, “pypuf: Cryptanalysis of Physically Unclonable Functions,” 2021. [Online]. Available: <https://doi.org/10.5281/zenodo.3901410>
- [49] O. Group, “Cva6 risc-v cpu,” 2024, accessed: November 2024. [Online]. Available: <https://github.com/openhwgroup/cva6>
- [50] N. Corporation, “Nvdl hardware: Open-source deep learning accelerator,” <https://github.com/nvdl/hw>, 2017, accessed: 2025-07-18.
- [51] UltraEmbedded, “Risc-v soc,” 2024, accessed: November 2024. [Online]. Available: https://github.com/ultraembedded/riscv_soc
- [52] “CVA6 RISC-V CPU.” [Online]. Available: <https://github.com/openhwgroup/cva6>
- [53] “or1200_soc.” [Online]. Available: https://opencores.org/projects/or1200_soc